

Muon Spin Rotation and Mössbauer Investigations of the Spin Transition in $[\text{Fe}(\text{ptz})_6](\text{ClO}_4)_2^\perp$

S. J. Campbell,^{†,‡} V. Ksenofontov,[†] Y. Garcia,^{†,§} J. S. Lord,^{||} Y. Boland,[§] and P. Gülich^{*,†}

Institut für Anorganische Chemie und Analytische Chemie, Universität Mainz, 55099 Mainz, Germany, School of Physical, Environmental and Mathematical Sciences, The University of New South Wales, Australian Defence Force Academy, Canberra, ACT 2600, Australia, Unité de Chimie des Matériaux Inorganiques et Organiques, Département de Chimie, Faculté des Sciences, Université Catholique de Louvain, Place L. Pasteur 1, 1348 Louvain-la-Neuve, Belgium, and ISIS, Rutherford Appleton Laboratory, Chilton, Didcot, OX11 0QX, UK

Received: July 17, 2003; In Final Form: October 24, 2003

The compound $[\text{Fe}(\text{ptz})_6](\text{ClO}_4)_2$ (ptz = 1-propyl-tetrazole) displays a gradual thermal spin crossover with magnetic susceptibility measurements ($\sim 4.2\text{--}300\text{ K}$) showing that the transition is centered around $T_{1/2} \sim 150\text{ K}$ and extends from $\sim 90\text{--}190\text{ K}$. Evidence of the scope to track a thermally induced spin transition using muon spin rotation (μSR) is provided in particular via the temperature dependence of the initial asymmetry parameter in the zero field as well as the relaxation rates. The spectral line broadening observed in the Mössbauer spectra of $[\text{Fe}(\text{ptz})_6](\text{ClO}_4)_2$ at $\sim 200\text{ K}$ is attributed to relaxation phenomena associated with the dynamics of the crystal lattice. Dynamic processes are also detected by μSR as revealed by the pronounced increase of the relaxation rate of a fast-relaxing component above 200 K . Muonium-substituted radicals delocalized on the tetrazole ring have been identified on the basis of applied magnetic field μSR experiments from 10 to 2000 Oe .

Introduction

Iron(II) spin crossover (SCO) materials represent an important class of switchable transition-metal compounds.¹ The spin state of these compounds can be addressed on the molecular scale from high-spin (HS, $S = 2$) to low-spin (LS, $S = 0$) by several perturbations including temperature, pressure, and electromagnetic radiation.² The family of mononuclear Fe(II) 1R-tetrazole compounds have been among the most-studied SCO systems during the past decade.^{2a,b} A variety of SCO behavior can be observed, ranging from smooth, hysteretic, incomplete, and even stepwise transitions.^{3–5} $[\text{Fe}(\text{ptz})_6](\text{BF}_4)_2$ (ptz = 1-propyl-tetrazole) is by far the best-known tetrazole compound whose spin transition (ST) has been thoroughly investigated using a wide range of physical techniques such as magnetic susceptibility measurements, differential scanning calorimetry, Mössbauer, UV–vis, NMR, and IR, among others.^{2–5} This material displays a hysteretic ST on cooling,² reflecting a crystallographic phase transition.^{6,7} Of particular interest is the finding (as demonstrated by a set of UV–vis experiments) that the ST triggers the accompanying crystallographic phase transition.⁶ This material was also the first to reveal a ST induced by light (light-induced excited spin state trapping),⁸ thus opening a new field of research for investigation.¹

By comparison, little attention has been directed to the perchlorate derivative, $[\text{Fe}(\text{ptz})_6](\text{ClO}_4)_2$.⁶ As shown in Figure 1, the iron(II) ion is octahedrally coordinated by six monodentate

1R-tetrazole ligands. The SCO cations and the noncoordinated perchlorate anions are arranged in electrically neutral layers with trigonal symmetry, linked by weak van der Waals interactions.⁹ Although the crystal structure reveals one crystallographic iron site,⁹ on cooling through the ST, intriguing line broadening was observed in the ^{57}Fe Mössbauer spectra.¹⁰ In addition, despite the absence of thermal hysteresis, the crystals were found to crack on cooling.¹¹ While this latter behavior could indicate a first-order structural phase transition, the line broadening could also be associated with the dynamic behavior of the octahedral iron complexes during the SCO process. We have applied the muon spin rotation (μSR) technique in order to obtain further microscopic information about the ST in $[\text{Fe}(\text{ptz})_6](\text{ClO}_4)_2$. In μSR spectroscopy, spin-polarized positive muons are implanted into a sample thereby acting as probes of the local magnetization.¹² While ^{57}Fe Mössbauer spectroscopy enables the local hyperfine fields at Fe lattice sites to be determined, positive muons mainly sense the interstitial sites and hence the dipolar fields generated by surrounding paramagnetic ions or bonds to the ligands when exchange coupling to the paramagnetic ions also contributes. This paper is concerned primarily with an extended μSR and ^{57}Fe Mössbauer study of $[\text{Fe}(\text{ptz})_6](\text{ClO}_4)_2$. A preliminary account of this work has been presented.¹³

Experimental Section

The ptz ligand was prepared by refluxing propylamine hydrochloride, sodium azide, and triethylorthoformate in acetic acid.¹⁴ $[\text{Fe}(\text{ptz})_6](\text{ClO}_4)_2$ was synthesized and characterized as described elsewhere⁹ using concentrated aqueous solutions of 1-propyltetrazole and $[\text{Fe}(\text{H}_2\text{O})_6](\text{ClO}_4)_2$ under nitrogen. The compound was recrystallized from dry nitromethane to give a hygroscopic crystalline material. **Caution: Perchlorate salts are potentially explosive and should be handled with care.** The

* Author to whom correspondence may be addressed. E-mail: guetlich@uni-mainz.de.

[†] Universität Mainz.

[‡] The University of New South Wales.

[§] Université Catholique de Louvain.

^{||} Rutherford Appleton Laboratory.

[⊥] Dedicated to Professor Bernt Krebs on the occasion of his 65th birthday.

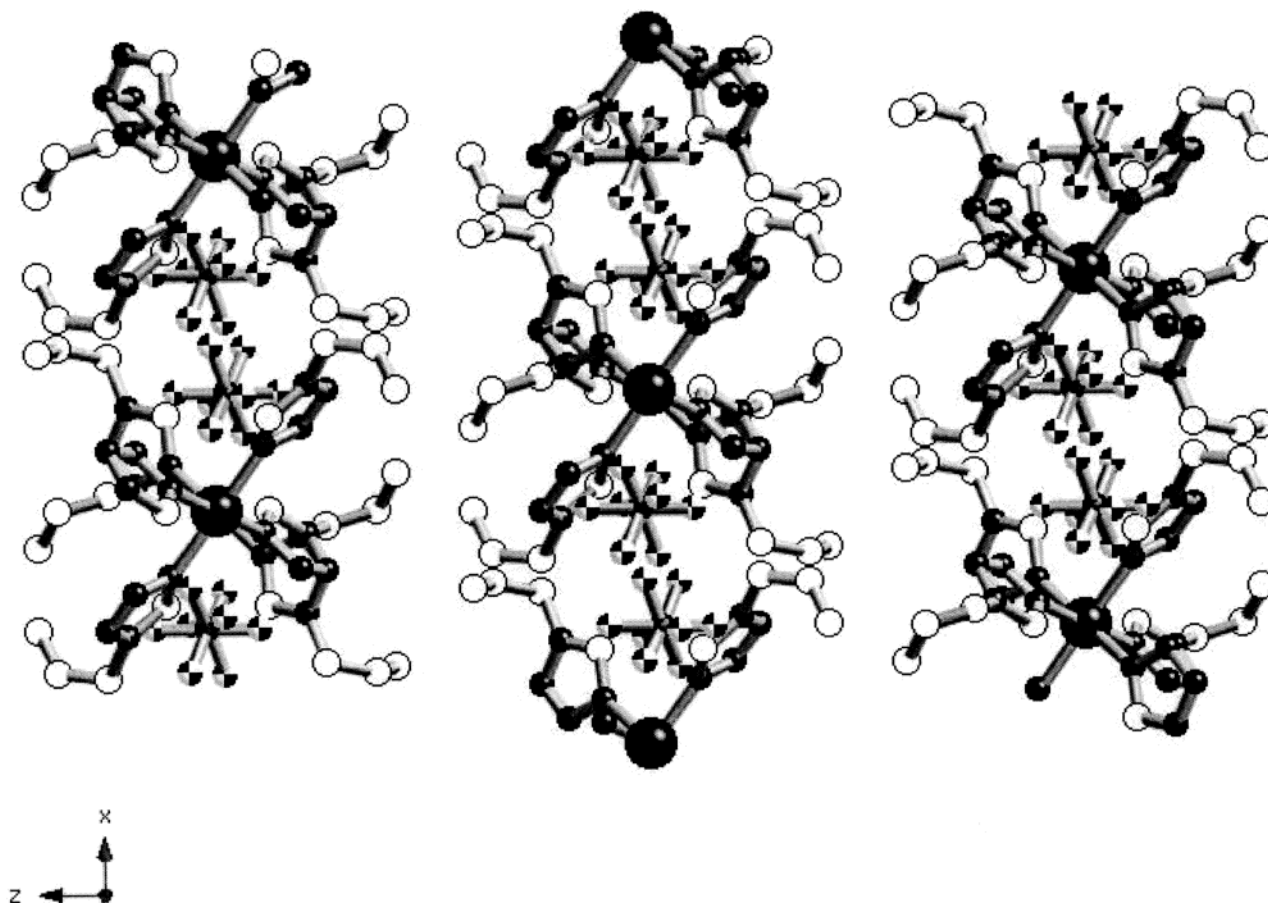


Figure 1. A view of the crystal lattice of $[\text{Fe}(\text{ptz})_6](\text{ClO}_4)_2$. Black, white, and black and white small spheres correspond to nitrogen, carbon, and oxygen atoms, respectively. The larger black spheres correspond to iron(II) ions.

^{57}Fe Mössbauer measurements were carried out using a conventional constant-acceleration spectrometer and helium cryostat and the spectra fitted using Recoil 1.03a Mössbauer Analysis Software.¹⁵ The magnetic susceptibility measurements (4.2–300 K) were carried out using a PAR 151 Foner-type magnetometer and a standard helium cryostat. Magnetic data were corrected for magnetization of the sample holder and for diamagnetic contributions, which were estimated from the Pascal constants. The μSR measurements were performed on the μSR spectrometer at ISIS, Rutherford Appleton Laboratory, UK. The muons with energy ~ 3.2 MeV and implantation ranges of the order of 100 mg cm^{-2} thermalize within the sample on time scales much shorter than the spin relaxation times. The muons decay with a mean lifetime of $2.2 \mu\text{s}$ and emit positrons preferentially in the direction of the muon spin. The positrons are detected by scintillation detectors surrounding the sample. The μSR spectra were recorded over the temperature range ~ 12 –300 K using a closed-cycle refrigerator.

Results

Magnetic and Mössbauer Measurements. The spin transition of $[\text{Fe}(\text{ptz})_6](\text{ClO}_4)_2$ is shown clearly by the magnetic susceptibility measurements in Figure 2. Here, $\chi_M T$ (the product of the molar magnetic susceptibility and temperature) remains approximately constant at $\sim 3 \text{ cm}^3 \text{ mol}^{-1} \text{ K}$ over the temperature range ~ 300 –190 K, consistent with the presence of only HS $\text{Fe}(\text{II})$ ions. $\chi_M T$ then gradually decreases down to $\sim 80 \text{ K}$, reaching a value indicative of LS $\text{Fe}(\text{II})$ ions. As shown in Figure 2, the compound demonstrates a gradual ST centered around $T_{1/2} \sim 150 \text{ K}$, which represents the temperature at which 50% of HS $\text{Fe}(\text{II})$ ions are present.

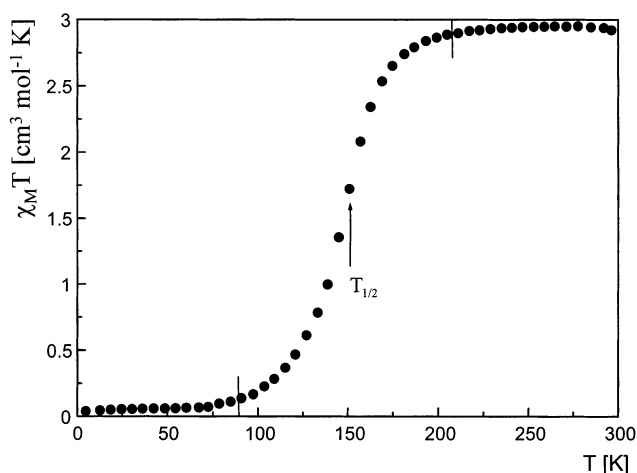


Figure 2. The temperature dependence of the molar susceptibility, $\chi_M T$, for $[\text{Fe}(\text{ptz})_6](\text{ClO}_4)_2$. The arrow indicates $T_{1/2} \sim 150 \text{ K}$ with the limits of the spin transition also marked.

Representative ^{57}Fe Mössbauer spectra as measured on cooling through the ST are shown in Figure 3. The spectrum at 270 K reveals one iron site with isomer shift and quadrupole splitting values of $\delta_{\text{HS}} = 1.07(1) \text{ mm s}^{-1}$ (relative to α iron) and $\Delta E_Q = 1.32(2) \text{ mm s}^{-1}$, respectively, which are characteristic of a HS $\text{Fe}(\text{II})$ ion. As can be discerned in the Mössbauer spectra, asymmetrical line broadening is found at 200 K, approximately 10 K before the onset of the ST at $\sim 190 \text{ K}$ as indicated by the magnetic measurements of Figure 2. Indeed, at 190 K a new resonance signal is observed corresponding to a LS $\text{Fe}(\text{II})$ ion. The Mössbauer spectrum at 125 K corresponds to an almost pure LS state with $\delta_{\text{LS}} = 0.55(1) \text{ mm s}^{-1}$ and ΔE_Q

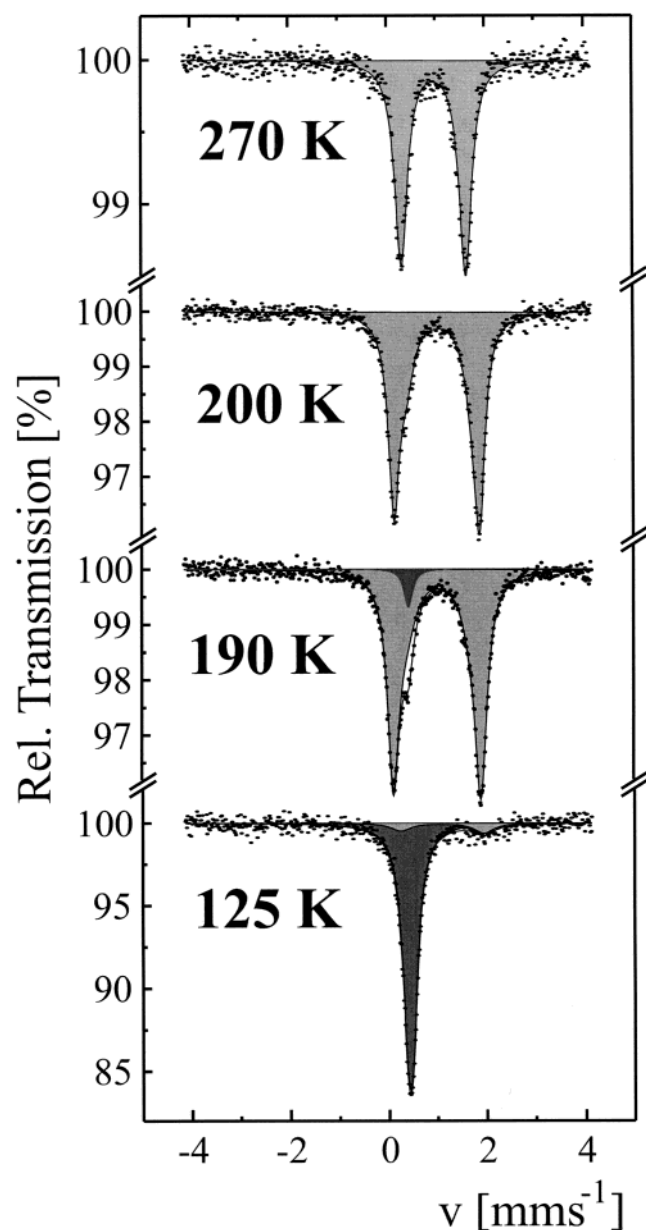


Figure 3. A set of representative ^{57}Fe Mössbauer spectra obtained on cooling $[\text{Fe}(\text{ptz})_6](\text{ClO}_4)_2$ through the region of the spin transition at $T = 270, 200, 190,$ and 125 K. The spectra have been fitted as described in the text with the predominant HS and LS subspectral components indicated. The shaded subspectra correspond to iron(II) (LS, dark gray) and iron(II) (HS, light gray).

$= 0.10(2) \text{ mm s}^{-1}$. This single line is characteristic of a highly symmetric local environment of the Fe(II) ion as found earlier for $[\text{Fe}(\text{ptz})_6](\text{BF}_4)_2$.³

Given the lack of evidence for a structural phase transition, the line broadening of the HS doublet at 200 K is expected to reflect dynamical processes in the crystal lattice. Comparison of this behavior with that observed in earlier SCO studies¹⁶ could be taken to indicate a dynamical nature of the SCO behavior in $[\text{Fe}(\text{ptz})_6](\text{ClO}_4)_2$. However, at 200 K such an effect would require a sizable population of both the HS and LS states; this is not the case at this temperature where the compound is primarily in the HS state. Rather, the line broadening is likely to reflect the dynamic character of the crystal lattice with, for example, an order–disorder phenomenon of the perchlorate anions¹⁷ resulting in changes of the iron–nitrogen ligation. It is interesting to note that such effects have been detected at ~ 199 K on $[\text{Fe}(\text{bi})_3](\text{ClO}_4)_2$ (bi = 2,2'-bi-2-imidazoline) on the

basis of detailed temperature-dependent ^{57}Fe Mössbauer measurements and X-ray powder diffraction studies.¹⁸ In the present study, however, we have restricted ourselves to a qualitative discussion of the Mössbauer relaxation phenomena with detailed insight to the dynamic behavior of $[\text{Fe}(\text{ptz})_6](\text{ClO}_4)_2$ provided by the μSR measurements.

Muon Spin Rotation Measurements. Sets of typical zero-field muon spin-relaxation spectra for $[\text{Fe}(\text{ptz})_6](\text{ClO}_4)_2$ above and below $T_{1/2} \sim 150$ K are shown in parts a and b of Figure 4, respectively. The relaxation spectra shown in Figure 4a reveal two contributions. First, a sharp decrease of the asymmetry parameter is observed from $\sim 20\%$ down to $\sim 14\%$ in the $2 \mu\text{s}$ range. This fast relaxation is followed by a slower relaxation behavior. These spectra above $T_{1/2}$ were thus fitted on the basis of two Lorentzian lines. The relaxation spectra shown in Figure 4b reveal a monotonic behavior, which was accurately fitted best taking into account two Lorentzian lines in the range ~ 12 – 150 K. We notice that the overall initial asymmetry parameter, a_0 , remains constant around 20% above $T_{1/2}$, whereas below $T_{1/2}$, it decreases from $\sim 17\%$ down to $\sim 10\%$ around 12 K. As shown in Figure 5, the temperature variation of a_0 for $[\text{Fe}(\text{ptz})_6](\text{ClO}_4)_2$ in zero field correlates well with the ST curve derived from the magnetic susceptibility measurements. To aid this comparison, the $\chi_M T$ values of Figure 2 have been normalized to the values of the asymmetry parameter above and below $T_{1/2}$. The asymmetry parameter remains approximately constant over the range from 300 to 175 K before slowly decreasing with the onset of the spin transition. A slight deviation in the overlap between the two curves is nevertheless observed in the region from ~ 50 – 125 K. This is considered to be likely due to a few HS spins remaining at low temperatures, and consequently, muons may interact not only with the nearest iron spin but also those from next-nearest sites in $[\text{Fe}(\text{ptz})_6](\text{ClO}_4)_2$. The value of the initial asymmetry parameter below 120 K (~ 10 – 12%) corresponds to that of diamagnetic muonium perturbed by the local nuclear moments of atoms and the local electric fields of the crystal matrix. Confirmation of the presence of diamagnetic muons follows from comparison of the low transverse field and zero-field relaxation curves measured at 12 K. These two curves have approximately the same initial asymmetry and similar relaxation rates, and the transverse field data show the characteristic precession frequency for the diamagnetic muon (135.5 MHz/T).

Relaxation spectra were also measured at longitudinal fields (10–2000 Oe) over the temperature range ~ 10 – 300 K in order to determine the manner in which the implanted muons stabilize in the $[\text{Fe}(\text{ptz})_6](\text{ClO}_4)_2$ sample. Figure 6 shows the variation of the initial asymmetry parameter with the magnetic field at selected temperatures. The general behavior is represented by a slight increase in a_0 below 50 Oe followed by a pronounced increase before a_0 saturates above ~ 1000 Oe. This increase in initial asymmetry with magnetic field, reaching saturation at high-field values, provides evidence for the formation of a paramagnetic state such as muonium $\text{Mu} = \mu^+\text{e}^-$, an analogue of the hydrogen atom. By comparison, in low values of the magnetic field, the presence of a fraction of paramagnetic muonium is not clearly revealed because of its very high relaxation rate. At large applied magnetic fields, any paramagnetic muonium present would be repolarized when the Larmor frequency of the electron exceeds the hyperfine coupling of an electron and a muon. These curves of initial asymmetry parameters as a function of a magnetic field (Figure 6) have been analyzed in order to extract the hyperfine coupling constant, A , over the temperature range $12 \text{ K} \leq T \leq 170 \text{ K}$ as

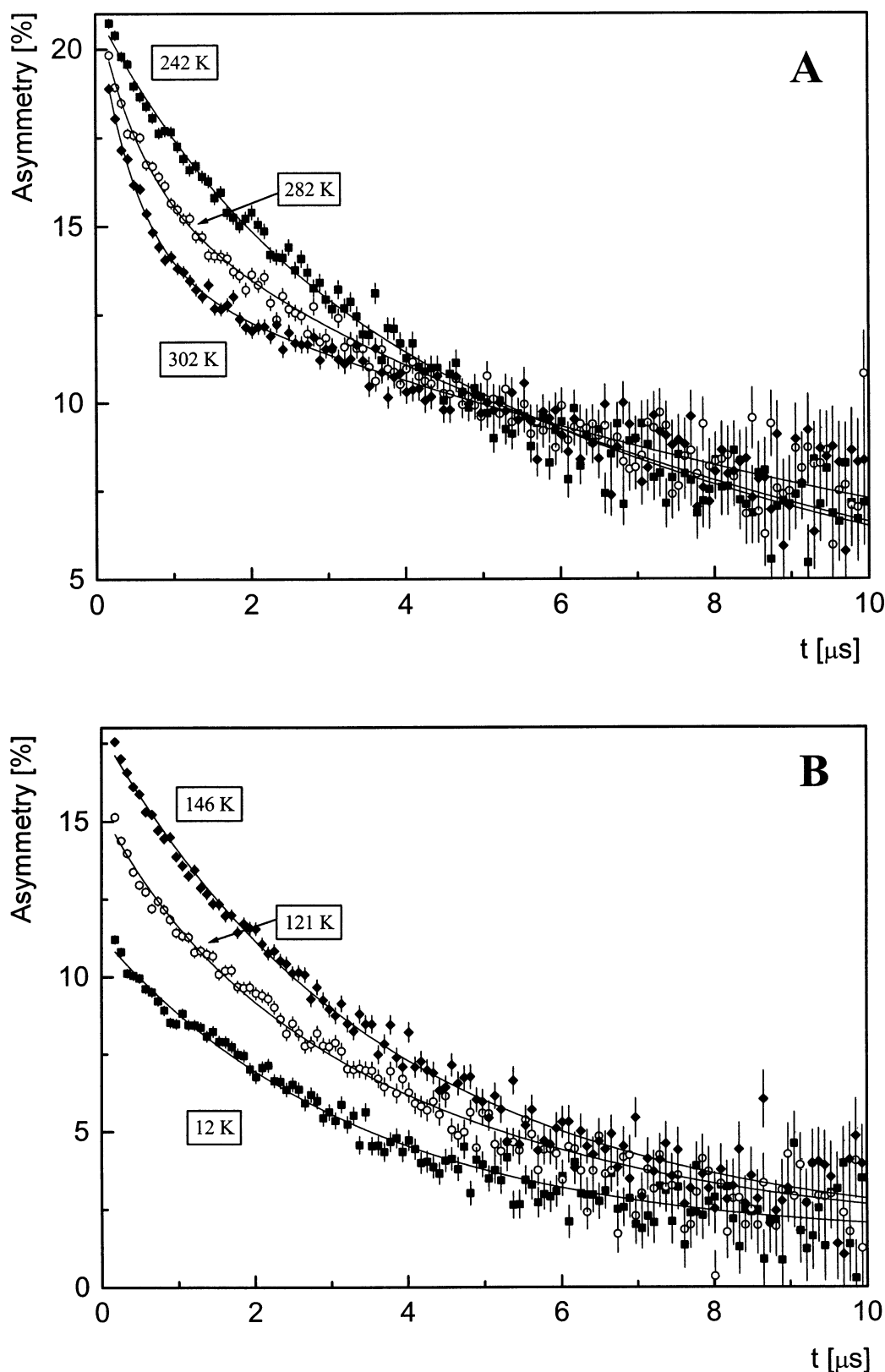


Figure 4. Representative zero-field muon spin-relaxation curves for $[\text{Fe}(\text{ptz})_6](\text{ClO}_4)_2$ at (A) above $T_{1/2} \sim 150$ K and (B) below $T_{1/2} \sim 150$ K.

follows. The muon relaxation spectra have been first analyzed for a range of fields at the same temperature to derive $a_0(B)$ which has been fitted, in a first approximation, to the following isotropic repolarization function¹⁹

$$a_0(B) = A_{\text{dia}} + A_{\text{para}} \left(1 + \frac{x^2}{x^2 + 1} \right) \quad (1)$$

where

$$x = (\gamma_e + \gamma_\mu) \frac{B}{A} \quad (2)$$

In eq 2, $\gamma_e = 28$ GHz/T, $\gamma_\mu = 135.5$ MHz/T, and A_{dia} and A_{para} represent the diamagnetic and paramagnetic contributions, respectively, in an applied field. The resultant value derived at

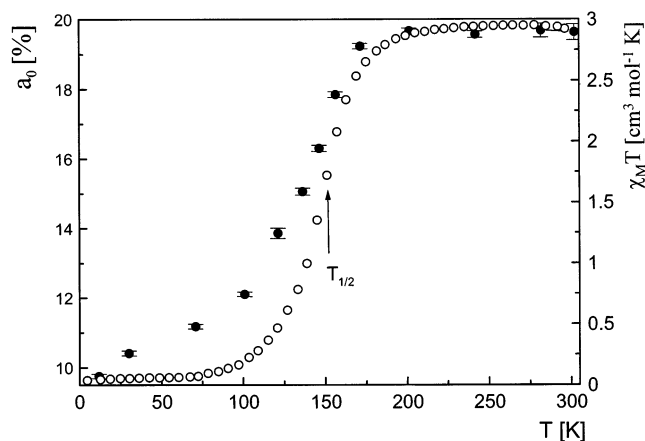


Figure 5. Comparison between the temperature dependence of $\chi_M T$ and the total asymmetry parameter in zero field for [Fe(ptz)₆](ClO₄)₂. The $\chi_M T$ values have been normalized to the values of the asymmetry parameter over the whole range of temperature.

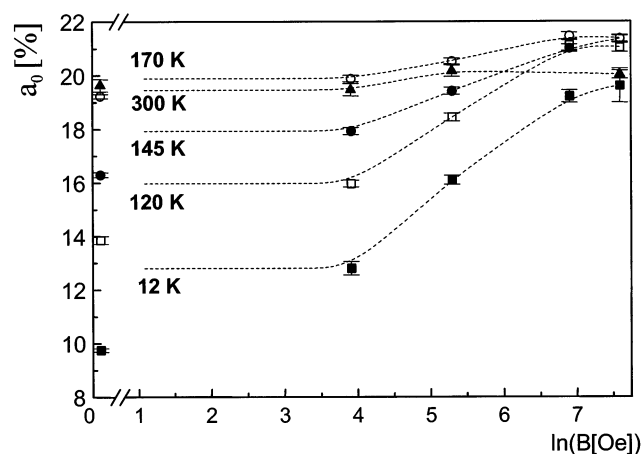


Figure 6. Dependence of the initial asymmetry parameter on the magnetic field at the temperature indicated. The curves are fits to the isotropic repolarization function, giving $A = 540 \pm 15$ MHz at ~ 12 K as discussed in the text.

~ 12 K, $A = 540 \pm 15$ MHz is typical of the hyperfine coupling constant for molecular radical states. By comparison, the hyperfine coupling constant for a free muonium atom is $A \sim 4400$ MHz.²⁰

Both the zero-field and longitudinal magnetic field muon-relaxation spectra were found to be fitted best with two Lorentzian components on the whole temperature range (~ 12 –300 K) using the following function

$$a(t) = a_s e^{-\lambda_s t} + a_f e^{-\lambda_f t} \quad (3)$$

where a_s and a_f represent the amplitude of the initial asymmetry of the slow and fast components, respectively; λ_s and λ_f are the decay constants of the slow and fast components, respectively. The amplitude of the slow component has been maintained at around 12% and allowed to increase slightly with temperature. The temperature dependences of the slow and fast components are shown in Figure 7. Below 120 K, the relaxation rates determined from the fits to the slow component are approximately constant with values of $\lambda_s \sim 0.15 \mu\text{s}^{-1}$. The λ_s values decrease slowly as the ST proceeds with increasing temperature, reaching slow relaxation rates of $\lambda_s \sim 0.06 \mu\text{s}^{-1}$ around room temperature. The fast component presents, however, a peculiar behavior. λ_f is approximately constant below 75 K at $\lambda_f \sim 0.7 \mu\text{s}^{-1}$; it then slowly decreases to $\sim 0.3 \mu\text{s}^{-1}$ at

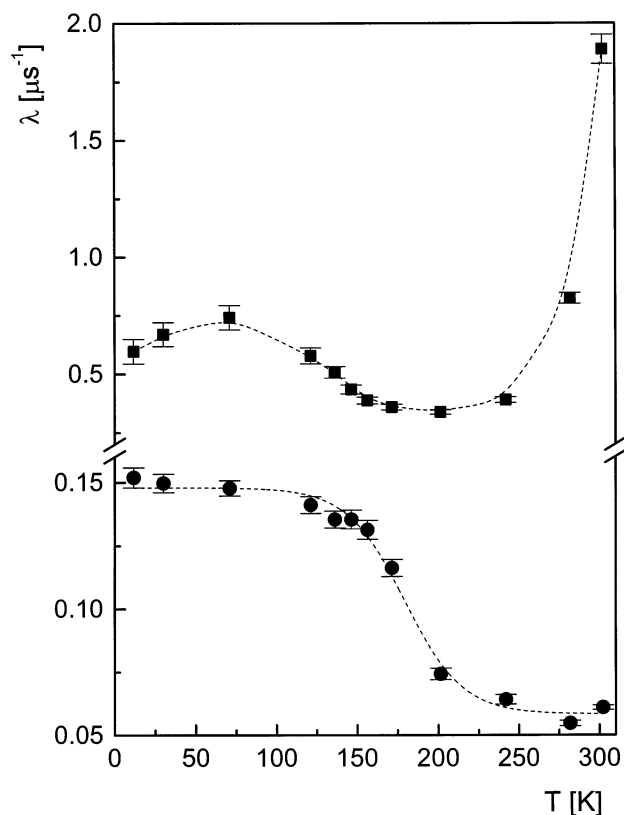


Figure 7. Temperature dependence of the slow (●) and fast (■) relaxation rate constants. The λ_s and λ_f values were determined as described in the text.

$T \sim 200$ K as the LS–HS transition proceeds before increasing rapidly at $T \sim 250$ K, reaching high values of $\lambda_f \sim 1.9 \mu\text{s}^{-1}$ at room temperature.

Discussion

While the behavior of SCO materials has been widely investigated using numerous physical techniques², μSR has only recently been applied in the study of the important transition from a HS state to a LS state.^{13,21,22} μSR measurements provide information about magnetic fluctuations and spin dynamics around a time window of $\sim 10^{-9}$ – 10^{-5} s and could be extremely useful in the study of the dynamics associated with spin transitions.²³

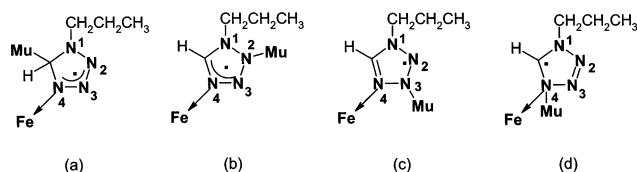
The overall temperature dependence of the initial asymmetry parameter of [Fe(ptz)₆](ClO₄)₂ can be considered as follows. The appearance of HS states in the temperature range of the SCO transition leads to their interaction with electronic spins of muonium. The response of the initial asymmetry parameter to an applied magnetic field above the transition temperature reveals a full asymmetry but with a weak dependence on magnetic field. This behavior provides evidence that apparently only diamagnetic-like muonium states as well as pure diamagnetic muons are present in the HS state of the compound. Also, the temperature dependence of the asymmetry parameter in the HS phase is also weak. An increase in the fraction of the diamagnetic muonium states can be understood if the dynamic character of paramagnetic spins in the HS phase, which are coupled strongly to the muonium electron, is considered. For $120 \text{ K} \leq T \leq 190 \text{ K}$, the iron spin and muonium electron spin are coupled and have a sufficiently high relaxation rate to decouple from the muon. As the temperature increases, the relaxation frequency of the spins of the iron complexes

increases. At high temperature ($T \geq 200$ K), electrons of muonium cannot follow fully the relaxation rate of the spins of the iron complexes, so their own relaxation rate falls and they begin to cause the muon to relax. This leads to the appearance of “fast” and “slow” parts on the muon relaxation curve. The “slow” part corresponds to diamagnetic muons and diamagnetic-like muonium as described above, whereas the “fast” part corresponds to muonium with electrons, in correlation with spins of iron complexes.

Of special interest is the predominant diamagnetic-like muonium fraction present in the HS state of $[\text{Fe}(\text{ptz})_6](\text{ClO}_4)_2$. The temperature dependence of the asymmetry parameter provides an indication of the fraction of the muons that interact with unpaired spins in the SCO compound and therefore the fraction of high spins present at any temperature. The similarity of the susceptibility and muon asymmetry curves (Figure 5) also suggests that either the muon radical only interacts with one neighboring Fe spin or that in the mixed state the HS and LS Fe ions are clustered rather than being randomly mixed.

The unusual diamagnetic behavior observed for the muons in the paramagnetic surroundings of the HS state of the SCO compound presumes a strong spin–spin interaction between the electron of the radical and the unpaired electrons of the SCO molecule in the HS state. This spin–spin interaction is greater than the strength of the muon hyperfine interaction²⁰ and causes the electron spin to fluctuate sufficiently rapidly to decouple it from the muon. Since we have diamagnetic and paramagnetic fractions at 300 K, the faster-relaxing component has extra relaxation $\lambda = \lambda_f - \lambda_s \sim 1.8 \mu\text{s}^{-1}$ because of its radical nature, giving an electron fluctuation rate of $\nu = A^2/\lambda \sim 250$ GHz at 300 K. The disappearance of unpaired spins during the SCO transition allows us to observe the paramagnetic radical state that interacts with the static internal magnetic fields created by the nuclear dipole moments of the lattice atoms.

In the present work, we have found evidence for the presence of muonium-substituted radicals in $[\text{Fe}(\text{ptz})_6](\text{ClO}_4)_2$. Muonium is preferentially located on an atom at the end of a double bond, with the unpaired electron spin located mainly on the other end.^{24,25} As depicted below, four different locations for the muonium in ptz can therefore be suggested, bonded to the C atom or bonded to the nitrogen atoms N2, N3, or N4.



The bonding of the muonium to the carbon atom (a) or to N2 (b) leads to an unpaired electron which is delocalized on three atoms of the ring due to the unsaturated character of muonated ptz. A similar situation can be found for instance for the addition of muonium on heterocycles such as furan²⁶ or 1-methylimidazole.²⁷ These two muonated forms, (a) and (b), are indeed more stable than the one found when the muonium is bonded to N3 (c), which gives a localized unpaired electron spin on N2. The bonding of muonium to N4 (d) would require the muon to be close to the Fe ion, which is unlikely for steric reasons. Also, a decrease of the crystal field strength that should stabilize the HS state is expected, but such an effect is not observed. Rather a clear correlation between the magnetic data and the thermal variation of the μSR initial asymmetry parameter in zero field has been found. The positions proposed for the muonium could be tested using density functional calculations

to simulate the muonium-substituted radicals, along with transverse field measurements.

The characteristic observation time of a Mössbauer experiment of 4×10^{-8} s is comparable with the observation time of muonium in μSR ($\sim 10^{-9}$ s). In $[\text{Fe}(\text{ptz})_6](\text{ClO}_4)_2$, the increase of the relaxation rate of the fast component detected above 200 K by μSR (see, e.g., Figures 4a and 7) is consistent with the observation of dynamic processes in the crystal lattice. These fast processes are not expected to involve the anionic sublattice, however, as the possibility of muonium being attached to the perchlorate anions is unlikely as these entities are not hydrogen bonded in this material. The order–disorder transition of the perchlorate anions is, however, clearly revealed by ^{57}Fe Mössbauer spectroscopy, with the observation of a line broadening of the spectra at ~ 200 K (Figure 3).

Conclusions

The spin transition occurring in the mononuclear iron(II) complex, $[\text{Fe}(\text{ptz})_6](\text{ClO}_4)_2$, has been characterized by superconducting quantum interference device and Mössbauer spectroscopy measurements. The ST curve has been delineated using μSR via the temperature dependence of the initial asymmetry parameter and the relaxation rate constants for the first time. Muonium formation has been identified and is likely to be delocalized on the tetrazole ring. We have also shown that ^{57}Fe Mössbauer and μSR spectroscopy are two independent and complementary methods in revealing the dynamic nature of the HS state in $[\text{Fe}(\text{ptz})_6](\text{ClO}_4)_2$. Indeed, the dynamical nature of the interaction between spins of muonium and of the iron(II) complex has been discussed and compared to the dynamics of the anionic sublattice of $[\text{Fe}(\text{ptz})_6](\text{ClO}_4)_2$ observed by Mössbauer spectroscopy. Extended μSR measurements of further sets of characteristic SCO molecular materials are in progress.

Acknowledgment. S.J.C. acknowledges renewal of an Alexander von Humboldt Research Fellowship while at the Johannes Gutenberg-Universität, Mainz, and support from the Access to Major Research Facilities Program, Australian Nuclear Science and Technology Organization. We acknowledge support from the European Union under Framework 5 for access to the MUSR instrument at the ISIS Facility, Rutherford Appleton Laboratory, U.K., and support from the European Commission for granting Contract No. ERB-FMRX-CT98-0199EEC/TMR. We also gratefully acknowledge the financial help from the Fonds der Chemischen Industrie and the Materialwissenschaftliches Forschungszentrum der Universität Mainz. We thank the Fonds National de la Recherche Scientifique for supporting a training period at the ISIS facility for Y.B. and the Fonds pour la Formation à la Recherche dans l’Industrie et dans l’Agriculture for a doctoral scholarship (Y.B.). We thank S. Reiman for recording the Mössbauer spectra.

References and Notes

- Gütlich, P.; Garcia, Y.; Woike, Th. *Coord. Chem. Rev.* **2001**, 219–221, 839.
- (a) Gütlich, P.; Hauser, A.; Spiering, H. *Angew. Chem., Int. Ed. Engl.* **1994**, 33, 2024. (b) Gütlich, P.; Spiering, H.; Hauser, A. In *Inorganic Electronic Structure and Spectroscopy*; Solomon, E. I., Lever, A. B. P., Eds.; John Wiley and Sons, Inc.: New York, 1999; Vol. 2, p 575. (c) Gütlich, P.; Garcia, P.; Goodwin, H. A. *Chem. Soc. Rev.* **2000**, 29, 419.
- Müller, E. W.; Ensling, J.; Spiering, H.; Gütlich, P. *Inorg. Chem.* **1983**, 22, 2074.
- Buchen, Th.; Gütlich, P. *Chem. Phys. Lett.* **1994**, 220, 262.
- Stassen, A. F.; Dova, E.; Ensling, J.; Schenk, H.; Gütlich, P.; Haasnoot, J. G.; Reedijk, J. *Inorg. Chim. Acta* **2002**, 335, 61.
- Jung, J.; Bruchhäuser, F.; Feile, R.; Spiering, H.; Gütlich, P. *Z. Phys. B* **1996**, 100, 517.

- (7) Moritomo, Y.; Kato, K.; Nakamoto, A.; Kojima, N.; Nishibori, E.; Takata, M.; Sakata, M. *J. Phys. Soc. Jpn.* **2002**, *71*, 1015.
- (8) Decurtins, S.; Gütllich, P.; Köhler, C. P.; Spiering, H.; Hauser, A. *Chem. Phys. Lett.* **1984**, *105*, 1.
- (9) Wiehl, L. *Acta Cryst.* **1993**, *B49*, 289.
- (10) Poganiuch, P. Ph.D. Dissertation, University of Mainz, Germany, 1989.
- (11) Schmitt, G. Ph.D. Dissertation, University of Mainz, Germany, 1996.
- (12) (a) Blundell, S. J. *Philos. Trans. R. Soc. London, Ser. A* **1999**, *357*, 2923. (b) Blundell, S. J. *Contemp. Phys.* **1999**, *40*, 175. (c) Muon Science: Muons in Physics, Chemistry and Solids, (Eds. Lee, S. L.; Kilcoyne, S. H.; Cywinski, R.) Proc. of the 50th Scottish University Summer School in Physics, A Nato Advanced Study Institute, Institute of Physics, Vol. 51, 1998.
- (13) Campbell, S. J.; Ksenofontov, V.; Garcia, Y.; Lord, J. S.; Reiman, S.; Gütllich, P. *Hyperfine Interact. C* **2002**, *5*, 363.
- (14) Kamiya, T.; Saito, Y. *Ger. Offen.* P2147023.5, 1971.
- (15) Lagarec, K.; Rancourt, D. G. Recoil, Mössbauer Spectral Analysis Software for Windows 1.0; Department of Physics, University of Ottawa.
- (16) Adler, P.; Spiering, H.; Gütllich, P. *Inorg. Chem.* **1987**, *26*, 3840.
- (17) Deszi, L.; Keszthelyi, L. *Solid State Commun.* **1966**, *4*, 511.
- (18) König, E.; Ritter, G.; Kulshreshtha, S. K.; Nelson, S. M. *Inorg. Chem.* **1982**, *21*, 3022.
- (19) Cox, S. F. J. *J. Phys. C: Solid State Phys.* **1987**, *20*, 3187.
- (20) Casperson, D. E.; Crane, T. W.; Denison, A. B.; Egan, P. O.; Hughes, V. W.; Mariam, F. G.; Orth, H.; Reist, H. W.; Souder, P. A.; Stambaugh, R. D.; Thompson, P. A.; Putlitz, G. *Phys. Rev. Lett.* **1977**, *38*, 956.
- (21) Shioyasu, N.; Kagetsu, K.; Mishima, K.; Kubo, M. K.; Tominaga, T.; Nishiyama, K.; Nagamine, K. *Hyper. Interact.* **1994**, *84*, 477.
- (22) Blundell, S. J.; Pratt, F. L.; Lancaster, T.; Marshall, I. M.; Steer, C. A.; Hayes, W.; Sugano, T.; Letard, J.-F.; Caneschi, A.; Gatteschi, D.; Heath, S. L. *Physica B* **2003**, *326*, 556.
- (23) König, E. *Struct. Bond.* **1991**, *76*, 51.
- (24) Walker, D. C. *Muon and muonium chemistry*; Cambridge University Press: New York, 1983.
- (25) Roduner, E. *Chem. Soc. Rev.* **1993**, *22*, 337.
- (26) Percival, P. W.; Kiefl, R. F.; Kreitzman, S. R.; Garner, D. M.; Cox, S. F. J.; Luke, G. M.; Brewer, J. H.; Nishiyama, K.; Venkateswaran, K. *Chem. Phys. Lett.* **1987**, *133*, 465.
- (27) Rhodes, C. J.; Roduner, E. *J. Chem. Soc., Faraday Trans.* **1991**, *87*, 1497.